Bilingual Peptide Nucleic Acids: Encoding the Languages of Nucleic Acids and Proteins in a Single Self-Assembling Biopolymer

Colin S. Swenson, Arventh Velusamy, Hector S. Argueta-Gonzalez, Jennifer M. Heemstra*

Department of Chemistry, Emory University, Atlanta, Georgia 30322, USA
*Correspondence:
jen.heemstra@emory.edu

Abstract:

Nucleic acids and proteins are the fundamental biopolymers that support all life on Earth. Nucleic acids store large amounts of information in nucleobase sequences while peptides and proteins utilize diverse amino acid functional groups to adopt complex structures and perform wide-ranging activities. Although Nature has evolved machinery to read the nucleic acid code and translate it into amino acid code, the extant biopolymers are restricted to encoding amino acid or nucleotide sequences separately, limiting their potential applications in medicine and biotechnology. Here we describe the design, synthesis, and stimuli-responsive assembly behavior of a bilingual biopolymer that integrates both amino acid and nucleobase sequences into a single peptide nucleic acid (PNA) scaffold to enable tunable storage and retrieval of tertiary structural behavior and programmable molecular recognition capabilities. Incorporation of a defined sequence of amino acid side-chains along the PNA backbone yields amphiphiles having a “protein code” that directs self-assembly into micellar architectures in aqueous conditions. However, these amphiphiles also carry a “nucleotide code” such that subsequent introduction of a complementary RNA strand induces a sequence-specific disruption of assemblies through hybridization. Together, these properties establish bilingual PNA as a powerful biopolymer that combines two information systems to harness structural responsiveness and sequence recognition. The PNA scaffold and our synthetic system are highly generalizable, enabling fabrication of a wide array of user-defined peptide and nucleotide sequence combinations for diverse future biomedical and nanotechnology applications.

Introduction:

Nature encodes information, structure, and function in two basic forms of biopolymers: nucleic acids and proteins. Nucleotide sequences in DNA or RNA encode both genetic information and complementary molecular recognition properties, while amino acid sequences in peptides and proteins convey complex information for structure and function. The robust and adaptable performance of both of these biopolymer structures has been a fundamental driving force for evolution on Earth and explains their continued ubiquitous presence in Nature. Moreover, the straightforward design principles and privileged physicochemical properties of both nucleic acids and proteins position them as attractive materials to leverage and integrate in applications beyond their canonical roles.[1–3] For example, combining the high density of negative charge of DNA molecules with hydrophobic lipids or organic polymers enables assembly and formation of complex nanostructures including micelles, tubes, and vesicles.[4–6] While these DNA-polymer conjugates successfully integrate structural responsiveness and can perform sequence-specific recognition, they are difficult to control in biological systems and are limited to anionic backbones. Conversely, peptides are able to express myriad biophysical characteristics through programmable amino acid side-chain functionalities but lack the vast information storage and highly modular molecular recognition capabilities of nucleic acids. The ability to combine the functional properties of nucleic acids and proteins into a single biomolecule would largely overcome these material limitations. A “bilingual” biopolymer, able to simultaneously speak both amino acid and base-pairing languages, would allow for both the information processing capability of nucleobase sequence recognition as well as the structural and functional versatility afforded to peptides and proteins, together creating a powerful tool for biomedical and nanotechnology applications.

Despite these clear advantages, uniting these two chemical functionalities presents a significant logistical challenge. We recognized that peptide nucleic acid (PNA) offered an ideal scaffold for the design of a bilingual biopolymer, as is it capable of storing sequence-specific

nucleotide code along a neutral pseudopeptide backbone.[7–9] This backbone imparts a number of desirable properties including extremely high affinity for complementary nucleic acids, enhanced stability in complex biological environments, and most significantly, the ability to incorporate amino acid side-chains at sequence-defined positions.[10–12] Researchers have used the latter capability to impact properties such as solubility, cell permeability, enhanced base-pairing, and bioconjugation.[13–22] Additionally, PNA-polymer conjugates have been constructed and shown to self-assemble.[23–25] While these are capable of binding to complementary nucleic acids, the hydrophobic portion and nucleic acid code exist in different blocks of the polymer and thus hybridization cannot be used to control assembly. In contrast to these previous examples, integrating a complex amino acid sequence in the PNA backbone to encode assembly or conformational information has yet to be explored. We hypothesized that strategically placing hydrophobic or hydrophilic amino acid side-chains would enable us to controllably induce self-assembly of amphiphilic structures (**Figure 1**). We further speculated that addition of a complementary DNA or RNA strand would result in duplex formation with the PNA strand and a dramatic change in amphiphilicity, effectively harnessing the nucleic acid code to direct disruption of the assemblies. Here we demonstrate the design, synthesis, and characterization of such an amphiphilic PNA sequence and show assembly into micellar architectures under aqueous conditions. We also show stimuli-responsive disassembly using miRNA-21, a disease-related

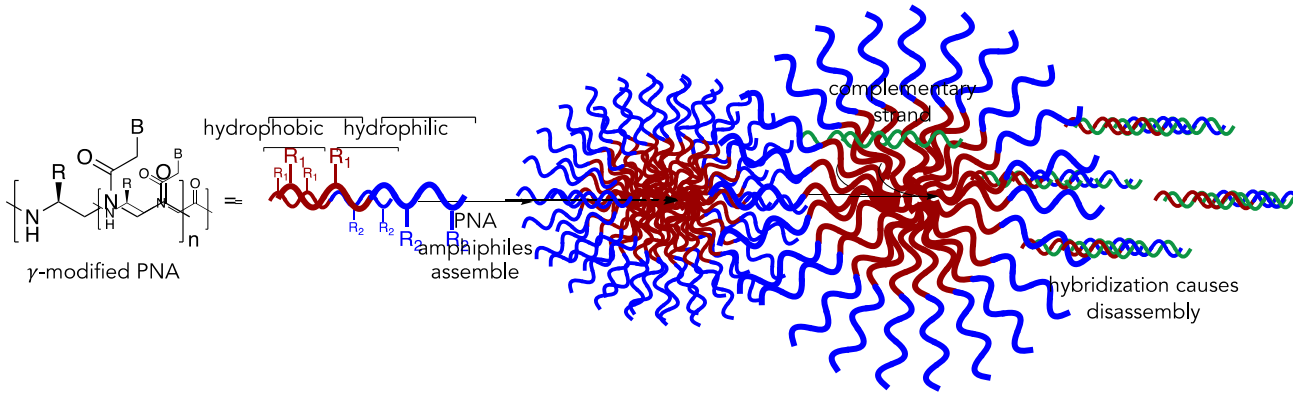

Figure 1: Schematic representation of bilingual PNA biopolymer. Amino acid side-chains at the γ-position direct assembly, and disassembly is triggered by recognition of the nucleobase code by a complementary DNA or RNA strand.

RNA target.[26] Together, these results represent the first example of a bilingual biopolymer capable of simultaneously encoding both amino acid and nucleotide information for utilization in controlled assembly and sequence-specific recognition.

Results and Discussion:

Design and Synthesis of Amphiphilic PNA

To demonstrate the ability of PNA to function as a bilingual biopolymer, we aimed to create a strand having a nucleobase sequence capable of specific RNA recognition and an amino acid sequence to impart amphiphilic behavior to drive assembly, analogous to folding or quaternary assembly of proteins. As a biologically relevant target, we designed a 12-nucleotide sequence complementary to miRNA-21, a well characterized oncomiR that is upregulated in almost all cancer types.[26] Conveniently, this complementary sequence exhibits low overall purine content and contains a single guanine nucleobase, averting sequence motifs that are known to be problematic in PNA synthesis and hybridization (**Table 1, Figure 2A**).[27] To impart hydrophobic properties in our amino acid sequence, we selected an alanine side-chain, as we previously observed aggregation of PNA having three methyl side-chains. For the hydrophilic portion of the sequence, we chose a positively-charged lysine side-chain, which afforded convenient synthetic access and is known to impart favorable solubility properties.[12,28] The side-chains were placed at

Table 1: Sequences of amphiphilic PNA-A, control PNA-C, and amino acid containing PNA-aa. "D" (orange) denotes the 4-DMN dye monomer. Subscripts denote the amino acid single letter code. Alanine monomers are in red. Lysine monomers are in blue. Masses were confirmed by ESI-TOF mass spectrometry.

Strand	Sequence	Mass $(M+3)^{3+}$	Found $(M+3)^{3+}$
PNA-A	C – D C T_A G A C_A T A C A_K A C T_K – N	1254.9174	1255.5575
PNA-C	C – Lys^+ D C T G A C T A C A A C T – N	1240.5718	1241.5304
PNA-aa	C – Ala Ala D C T G A C T A C A A C T Lys^+ Lys^+ – N	1330.2502	1331.6610

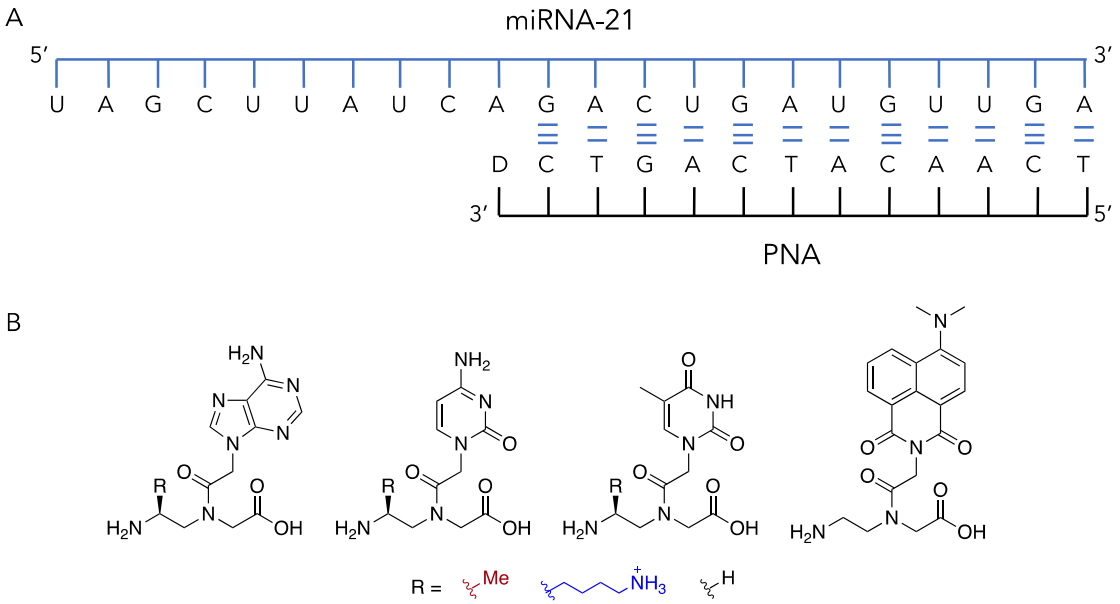

Figure 2: (A) Hybridization site of PNA oligomers to the miRNA-21 target used in this study. (B) PNA monomers synthesized in this study: γ-methyl monomers of cytosine and thymine, γ-lysyl monomers of adenine and thymine, and a solvatochromic 4-DMN monomer.

the γ-position along the PNA backbone using L-amino acids, as this enables installation of the side-chains using amino acid precursors, and this location and stereochemistry have been shown to confer increased binding affinity of PNA with complementary nucleic acids (**Figure 1**).[12,13] Lastly, we integrated a solvatochromic fluorophore, 4-dimethylamino-naphthalimide (4-DMN), at the hydrophobic terminus of the PNA (**Figure 2B**). This dye exhibits an enhancement in fluorescence intensity in increasingly hydrophobic environments,[29] and we envisioned that such an arrangement in the hydrophobic portion would allow us to visualize assembly formation by fluorescence spectroscopy.

We first synthesized the necessary γ-modified PNA monomers according to previously reported procedures.[22,28,30–32] Starting from Fmoc-protected L-amino acids, PNA backbones containing lysine and alanine side-chains were produced. The γ-modified backbones were coupled to bis(Boc)-protected nucleobase acetic acids using HATU in the presence of *N*-*N*-diisopropylethylamine (DIPEA) to produce γ-modified monomers of A, T, and C (**Scheme 1**). Synthesis of the 4-DMN PNA monomer was performed using a protocol adapted from that of Saito

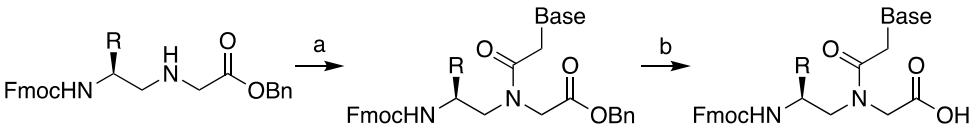

1: R = Lysyl; Base = A **3:** R = Me; Base = C

2: R = Lysyl; Base = T **4:** R = Me; Base = T

Scheme 1: General coupling procedure for the synthesis of γ-modified PNA monomers. (a) Nucleobase acetic acid, HATU, DIPEA, DMF; (b) H_2, Pd/C, MeOH.

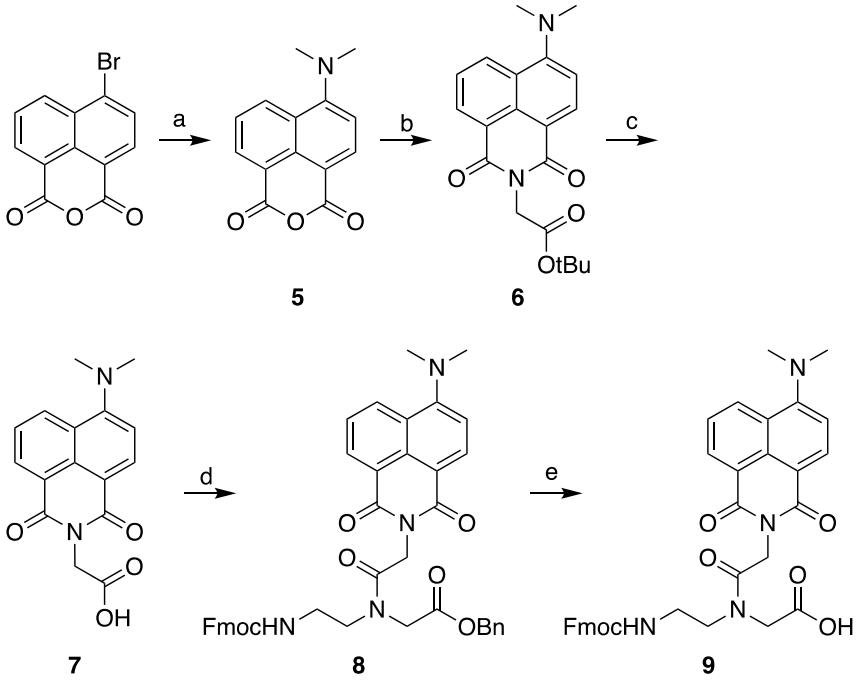

Scheme 2: Synthesis of 4-DMN PNA monomer. (a) 3-(dimethylamino)propionitrile, isoamyl alcohol, reflux, quant. (b) Glycine *tert*-butyl ester hydrochloride, DIPEA, DMF, 78%. (c) H_2, Pd/C, methanol, 94%. (d) Fmoc (aminoethyl)glycine benzyl ester, HATU, DIPEA, DMF, 72%. (e) H_2, Pd/C, methanol, quant.

and coworkers.[33] First, 4-dimethylamino-naphthalic anhydride was generated by reaction of 4-bromo-1,8-naphthalic anhydride with 3-dimethylamino-propionitrile in isoamyl alcohol.[34] The imide was then produced by condensation with glycine *tert*-butyl ester hydrochloride in the presence of DIPEA.[35] Removal of the tert-butyl protecting group by hydrolysis afforded the 4-DMN acetic acid. Unmodified (glycine) PNA backbone was synthesized according to previously reported procedure,[36] and the 4-DMN acetic acid was coupled to the unmodified backbone using HATU/DIPEA conditions to afford the 4-DMN PNA monomer (**Scheme 2**).

Amphiphilic PNA and control PNA oligomers were then produced using solid-phase synthesis employing HATU/DIPEA coupling conditions on a semi-automatic synthesizer with microwave assistance. Initially, we sought to place three hydrophobic side-chains and three hydrophilic side-chains equally spaced along the backbone. However, we were unable to obtain full-length product with this design. We hypothesized that this was due to the close proximity of semi-consecutive γ-modified monomers, which could severely lower the efficiency of the coupling reactions, resulting in little to no product formation. With this in mind, we reduced the number of γ-modified monomers to two alanine and two lysine side-chains. This design allowed placement of at least two unmodified monomers between each γ-modified residue, thereby mitigating otherwise poor coupling yields due to steric strain. Using this design, we produced an amphiphilic PNA sequence, PNA-A, as well as an unmodified control strand, PNA-C, containing a single C-terminal lysine, as is typically used in PNA strands to ensure solubility. In order to demonstrate the importance of using γ-modified monomers to encode the amino acid sequence along the PNA backbone, we also synthesized a control amphiphilic PNA, PNA-aa. This PNA has two alanine amino acids and two lysine amino acids on the C- and N-termini, respectively, and thus represents a sequence that is amphiphilic, but not bilingual, as the nucleotide and amino acid codes exist in separate blocks of the polymer (**Table 1).** The strands were purified via reverse-phase HPLC and characterized by ESI-TOF mass spectrometry to confirm identity (**Supporting Information**).

After synthesis and characterization of the PNA sequences, we performed UV melting experiments to analyze the hybridization of each sequence to a complementary DNA or the miRNA-21 target. The presence of side chains at the γ-position is known to increase the duplex stability of PNA to complementary nucleic acids.[13,14,21] Thus, we were not surprised to find that the complementary DNA exhibits a melting temperature (T_m) of 69.5 °C with PNA-A, compared to 63.0 °C and 64.5 °C for PNA-C and PNA-aa, respectively (**Figure S1A**). miRNA-21 also displays a higher T_m of 68.6 °C with PNA-A, compared to 65.8 °C and 67.5 °C for PNA-C and PNA-aa,

respectively, demonstrating that our γ-modifications improve the binding stability to complementary sequences (**Figure S1B**).

Characterization of Amphiphilic PNA Assembly

The ability of proteins to form tertiary and quaternary structures based on the information encoded in their primary amino acid sequence is a powerful tool. We envisioned that we could mimic this characteristic of proteins by encoding an amphiphilic amino acid sequence into the PNA backbone. After synthesis and characterization of the PNA strands, we sought to analytically confirm assembly formation and determine the critical micelle concentration (CMC) of PNA-A. To achieve this, we leveraged the ability of the 4-DMN dye to respond to changes in solvation, and we hypothesized that the dye's placement at the hydrophobic portion of the amphiphile should result in enhanced fluorescence upon assembly (**Figure 3A**).[29] CMC values determined using fluorescence-based methods often utilize a constant concentration of dye to visualize an inflection point where fluorescence increases. However, in our case the 4-DMN dye acts as an internal reporter, and thus changes in concentration as the concentration of amphiphile is varied. Given this approach, we instead quantified the relative fluorescence of PNA-A compared to the non-assembling dye monomer in solution. Indeed, we observed a concentration-dependent increase in fluorescence of amphiphile PNA-A over that of the 4-DMN monomer alone, suggesting the formation of assemblies having the dye sequestered in their hydrophobic core. Specifically we observe a discontinuous change in slope with increasing concentration, as is typical of micelle formation. In contrast, the control strand, PNA-C, displayed very little fluorescence enhancement with increasing concentrations, as it does not have an amino acid code to direct assembly (**Figure S2**). While PNA-C does show a small amount of fluorescence signal over the 4-DMN monomer alone, we surmise that this is attributable to the solvation state of the dye when placed near a hydrophobic nucleobase in the PNA strand, as opposed to the complete solvation of the free monomer. In any case, by observing the interception of the horizontal lower concentration and

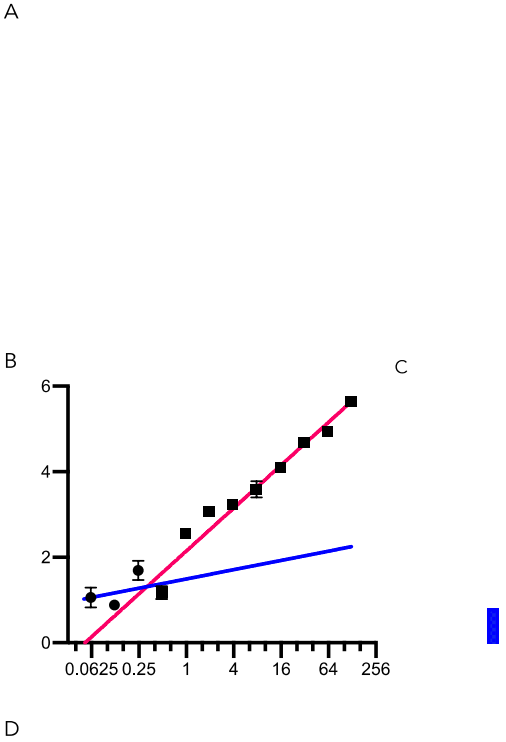

Figure 3: Characterization of amphiphilic PNA assembly. (A) Schematic representation of assembly and subsequent 4-DMN fluorescence response upon encapsulation. (B) Plot of the fluorescence ratio of PNA-A to the 4-DMN monomer as a function of concentration. Error bars represent SEM (n=3). (C) Histogram of the size distribution of particles as measured by ImageJ using TEM images. (D) TEM images of PNA-A at 100 μM. Scale bars = 2000 nm (top left), 1000 nm (top right), 500 nm (bottom left) and 50 nm (bottom right).

vertical upper concentration portions, we were able to estimate a CMC of ~317 nM, which is

sufficiently low for a broad range of stimuli-responsive biological applications (**Figure 3B**).

We next aimed to visually confirm the formation of assemblies and characterize their morphology using transmission electron microscopy (TEM). Amphiphile PNA-A was first dissolved in ultrapure water and diluted to a concentration of 100 μM. This solution was spotted onto formvar/carbon-coated copper grids and stained using a 1% uranyl acetate solution for TEM visualization. As expected, we observed the presence of spherical assemblies having an average diameter of 36.9 ± 9.9 nm, consistent with the formation of micelles (**Figure 3C-D**). Conversely, the PNA-C control strand displayed only a small number of amorphous assemblies, likely due to uncontrolled aggregation of PNA at this high of concentration or drying effects during sample preparation (**Figure S3**). The amino acid amphiphile, PNA-aa, displayed a heterogeneous mixture of amorphous assemblies, some having a similar size as the amphiphile PNA-A, but others being significantly larger, and all lacking discrete and uniform shapes (**Figure S4**). This may be explained by the flexibility of PNA-aa compared to PNA-A, as installing amino acid side-chains directly onto the PNA backbone at the γ-position results in the oligomer adopting a right-handed helical secondary structure that can be visualized via circular dichroism,[14] whereas including them outside of the nucleobases retains the flexibility of the backbone (**Figure S6**). Irrespective of the explanation, the ability of PNA-A, but not PNA-aa, to form well-defined assemblies demonstrates the unique capabilities of our bilingual biopolymers compared to other amphiphilic PNA conjugate designs.

In order to gain a better understanding of the assembly properties in solution, we also carried out analysis using dynamic light scattering (DLS). Samples of PNA were prepared at 500 μM, as lower concentrations failed to provide sufficient signal intensity for validated measurements. For the PNA-A assemblies, we observed a hydrodynamic diameter of 110.2 ± 31.9 nm according to the number distribution (**Figure S7**). This is larger than observed by TEM, but this difference is not entirely unexpected, as DLS has been shown to overestimate the sizes

of particles in solution because it is a measure of the hydrodynamic diameter as opposed to actual size.[37–39] Additionally, in TEM the sample is dried onto a surface during preparation, which may cause the assemblies to decrease in size. Finally, the high concentrations required for DLS may lead to the formation of some larger particles, increasing the average size observed. DLS analysis of PNA-aa reveals a similar trend, showing assemblies having a hydrodynamic diameter of 344.7 ± 92.3 nm (**Figure S7**), which is larger than the assemblies observed by TEM. The non-amphiphilic PNA-C shows two populations in DLS, with a significant population at 2.4 ± 0.5 nm and a small population at 54.9 ± 15.4 nm (**Figure S7**). The smaller sized population is consistent with single-stranded PNA while the larger may represent uncontrolled aggregation. This is in agreement with the TEM data, as only sparse and amorphous assemblies were visualized for the control PNA-C. Together, these results demonstrate our ability to encode amino acid information into a PNA sequence to direct the formation of organized nanostructures under aqueous conditions.

Stimuli-Responsive Switching of Amphiphilic PNA Assembly

Assembly of our PNA amphiphiles is driven by the amino acid code, and we envisioned that disassembly could be driven by the nucleotide code (**Figure 4A**). While we designed the amphiphilic PNA sequence to be responsive to miRNA-21, we used a complementary 12-nucleotide DNA strand in our initial disassembly studies owing to greater ease of use and lower cost. First, we sought to confirm the ability of the complementary DNA to bind to the amphiphilic PNA using circular dichroism (CD). Incorporating γ-modifications into PNA oligomers imparts chirality and orients the strand into a helical secondary structure, which can be observed by CD spectroscopy at concentrations relevant to assembly formation.[14] In order to detect PNA:DNA hybridization and subsequent disassembly, we first prepared PNA-A assemblies at 100 μM in 1x phosphate buffered saline (PBS), pH 7.4, as this concentration has previously displayed assemblies by TEM (**Figure 3D**). A range of concentrations of complementary or scrambled DNA

was added to the samples and CD signatures were recorded. We observed signals recording maxima near 263 nm and 222 nm, with minima occurring near 244 nm and 201 nm, which are indicative of a right-handed PNA:DNA duplex (**Figure 4B**).[14,40] As the concentration of complementary DNA in the samples was increased, the CD signal also increased while maintaining isosbestic points, suggesting a continuous increase in PNA:DNA duplex formation. Free DNA alone at 100 μM displayed maxima at 282 nm and 217 nm with minima occurring at 256 nm, further indicating that the increasing signal is caused by increased PNA:DNA duplex formation. As expected, we observed no increase in signal when PNA-A was exposed to the scrambled DNA sequence (**Figure 4D**). In fact, we observed a slight decrease in CD signal for PNA-A in the presence of scrambled DNA, which we speculate could be caused by minor electrostatic interference between the positively charged assemblies and the negatively charged DNA. We also confirmed that the control, PNA-C, and amino acid-containing amphiphile, PNA-aa, are capable of binding to complementary DNA at this concentration (**Figure S8**). Having established the ability of PNA-A to decode complementary DNA, we next aimed to explore whether similar decoding could be achieved using the full miRNA-21 target. Samples for CD spectroscopy were prepared as previously described at 100 μM but using only a single equivalent of RNA. We observed a significant change in CD signal, in particular a large increase in intensity at the 202 nm minima over that of PNA or miRNA alone, strongly suggesting the ability of the full target miRNA-21 to hybridize with PNA-A in water at concentrations relevant to assembly (**Figure 4F**).

Since our amphiphile is equipped with an internal fluorogenic dye, we sought to visualize disassembly via fluorescence response. Samples of PNA-A at 10 μM were prepared and mixed with increasing amounts of complementary and scrambled DNA. As expected, increasing amounts of complementary DNA caused the fluorescent signal to decrease (**Figure S9**). The change in fluorescence was not as significant as that observed via concentration-dependent

disassembly, likely because the dye can undergo base stacking with the hybridized DNA, still creating a somewhat hydrophobic environment. However, these data still provide evidence for DNA-induced disassembly. Interestingly, addition of the scrambled DNA sequence leads to an

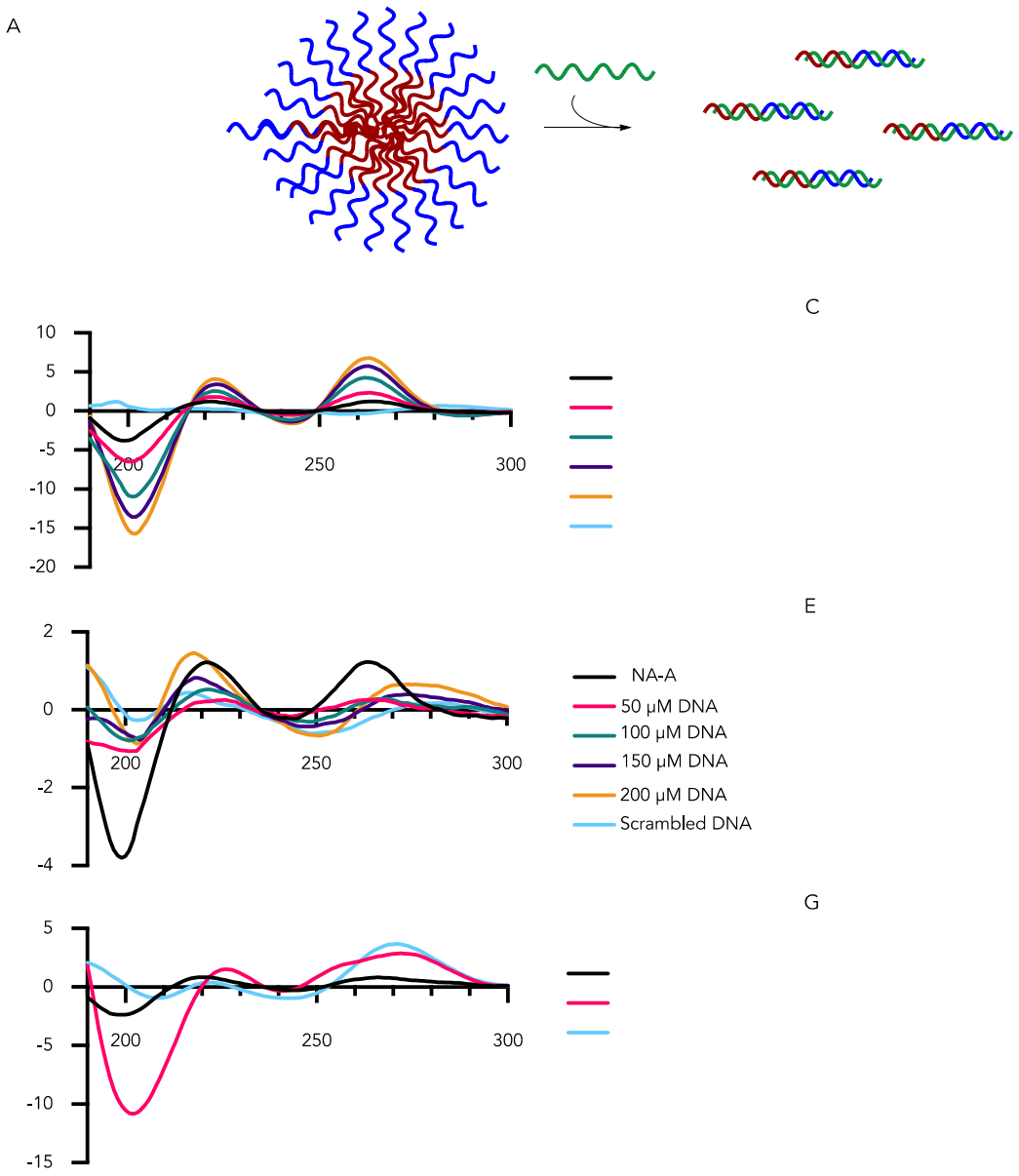

Figure 4: Binding and disassembly of amphiphilic structures by complementary nucleic acids. (A) Schematic representation of disassembly by hybridization of a complementary DNA or RNA strand. (B) CD plot confirming hybridization of complementary DNA to PNA-A in 1x PBS at 100 μM. (C) TEM image showing disappearance of spherical structures in the presence of complementary DNA. (D) CD plot showing inability of a scrambled DNA sequence to hybridize to PNA-A in 1x PBS at 100 μM. (E) TEM image showing retention of spherical assemblies in the presence of scrambled DNA. (F) CD plot confirming binding of full target miRNA-21 to PNA-A in water at 100 μM. (G) TEM image showing disappearance of spherical structures in the presence of complementary RNA. Scale bars in all TEM images = 500 nm.

increase in fluorescence signal. We hypothesize that this may result from non-specific interactions between the negatively charged DNA and the positively charged micelles, and that the resulting charge repulsion screening leads to compaction of the assemblies and thus a more hydrophobic environment in the micelle core.

While the fluorescence data are promising, we wanted to further validate and confirm disassembly using TEM. In order to visualize stimuli-responsiveness to DNA, amphiphile PNA-A assemblies were prepared at a concentration of 200 μM in 1x PBS. To these samples was added one equivalent of the complementary or scrambled DNA sequence to a final concentration of 100 μM. The samples were spotted onto grids and stained with uranyl acetate for TEM analysis. As expected, we observed the disappearance of spherical assemblies upon addition of the complementary DNA sequence, indicating stimuli-responsive disruption of the micelles (**Figure 4C**). As a control, we observed retention of small spherical nanostructures in the presence of non-targeting scrambled DNA, strongly indicating that sequence-specific binding is required for disassembly (**Figure 4E**). These assemblies appear to be slightly smaller than PNA-A alone, supporting our hypothesis for the fluorescence increase described above. We also detected some dark aggregates in the presence of both DNA sequences, and speculate this is likely due to the negative stain, uranyl acetate, which non-specifically interacts with phosphate ions present in the DNA backbone and PBS buffer, leading to precipitation. In any case, after confirming binding and stimuli-responsive disassembly by target DNA, we sought to also demonstrate responsiveness to the miRNA target of interest. Based on our previous results showing that one equivalent of DNA was sufficient for binding and disruption of assemblies, we challenged our PNA-A amphiphile constructs with a similar amount of miRNA-21. Assemblies were prepared in water and miRNA-21 was added to give final concentrations of 100 μM for both PNA and RNA. The samples were then spotted onto grids and stained with uranyl acetate for TEM visualization. As expected, we observed the disappearance of spherical assemblies in the presence of miRNA-21 (**Figure 4G**).

Consistent with our DNA studies, we observed similar staining precipitation patterns with miRNA-21, further suggesting that these objects are the result of non-specific artifactual precipitation between the uranyl acetate stain and phosphate-rich oligomers.

We had intended to also characterize disassembly using DLS, as this technique was successful for characterizing the assemblies in solution. However, as previously stated, this technique requires high concentrations (≥ 500 μM) of assemblies in order to obtain a reliable signal intensity.[37–39] At these concentrations, we observed the formation of a precipitate upon addition of the complementary target or a scrambled sequence. This is likely due to nonspecific electrostatic interactions which caused uncontrolled and catastrophic aggregation, resulting the presence of larger assemblies rather than the expected disappearance of assemblies. While lower concentrations do show the expected lack of assemblies, this may be attributable to insufficient signal and cannot necessarily be attributed to disassembly.

Together, the T_m, CD, fluorescence, and TEM results demonstrate that both DNA and RNA can bind sequence-specifically to PNA-A and disrupt assembly. Thus, even in the assembled state, the nucleotide code of our bilingual PNA constructs can be accessed and used to decode nucleic acid sequence information into supramolecular conformational changes. This property is similar to that shown in other PNA amphiphile systems.[23–25] However, these systems rely upon the addition of a hydrophobic alkyl chain and hydrophilic amino acids on opposite ends of the PNA oligomer to impart amphiphilic properties. While those designs are advantageous for ease of synthesis, our design is fundamentally different in that the entire portion of the amphiphile is capable of nucleobase-specific recognition. This allows greater control over the assembly and disassembly properties imparted by the amino acid and nucleobase codes, thus providing a truly modular bilingual biopolymer.

Conclusion:

Nature has evolved two languages for encoding the instructions and functions needed for life. While extant biopolymers are limited to encoding a single language, we introduce here a non-

natural biopolymer that is able to simultaneously encode both. We report the synthesis and characterization of a PNA strand having amino acid-like side-chains comprised of hydrophobic alanine and hydrophilic lysine, which when arrayed in a specific pattern are able to direct assembly in a manner analogous to peptide aggregation or quaternary protein assembly. The PNA strand also carries a specific nucleotide code, which is able to be decoded by complementary DNA or RNA to direct stimuli-responsive disassembly. These assembly and disassembly events can be observed both spectroscopically and using TEM, enabling characterization of the CMC and morphology of the assemblies and the sequence-specific nature of the disassembly process. The PNA scaffold is highly generalizable, allowing for the programming of both nucleotide and amino acid sequences to impart unique biological and physicochemical properties.[41] Thus, the ability of this information-rich bilingual biopolymer motif to undergo ordered self-assembly and conformationally respond to a variety of nucleic acid targets offers significant potential for applications in nanomedicine and biotechnology. While our initial exploration focused on micellar architectures, we envision that the bilingual biopolymer motif can be harnessed to recapitulate many of the structural motifs found in proteins, such as sheets and coils. Moreover, we anticipate that the ability to simultaneously interpret both of the biological codes can be extended beyond the creation of stimuli-responsive assemblies to also enable the construction of custom adaptors able to mediate precise interactions between specific protein and nucleic acid targets.

Experimental Procedures

Abbreviations: Fmoc, fluorenylmethyloxycarbonyl; DMF, dimethylformamide; HATU, 1-[Bis(dimethylamino)methylene]-1*H*-1,2,3-triazolo[4,5-*b*]pyridinium 3-oxid hexafluorophosphate; DIPEA, diisopropylethylamine; TFA, trifluoroacetic acid; DCM, dichloromethane; Boc, tert-butyloxycarbonyl; NMP, N-methyl-2-pyrrolidone.

PNA monomer synthesis

Unmodified PNA monomers were purchased from PolyOrg, Inc. Fmoc γ-lysyl and γ-methyl modified PNA backbones and nucleobase acetic acids of adenosine, thymine, and cytosine were prepared by previously published procedures.[22,28,30–32] Fmoc-L-amino acids and nucleobase starting materials were purchased from Chem-Impex International, Inc. All other reagents and solvents were purchased from Chem-Impex, Sigma-Aldrich, or Fisher Scientific and used without further purification unless otherwise stated. All dry solvents were distilled and collected from a J. C. Meyer solvent dispensing system prior to use to ensure dryness. Small molecule synthesis was monitored by thin layer chromatography (TLC) on Merck silica gel 60 F254 glass plates and visualized using UV light and staining with a ninhydrin solution followed by heating. Flash chromatography was performed using SiliaFlash F60 grade silica purchased from SiliCycle Inc. Compounds were characterized by proton magnetic resonance (^{1}H) and carbon nuclear magnetic resonance (^{13}C) NMR using a Varian Inova 400 MHz spectrometer containing a Bore Oxford magnet. Spectra were analyzed using the MestReNova software. The mass of compounds was confirmed by the use of an Agilent 6230 electrospray ionization time-of-flight (ESI-TOF) mass spectrometer.

General coupling procedure for PNA monomer synthesis

Nucleobase acetic acid (1 eq) was dissolved in dry DMF under N_2 in a round bottom flask. To the flask was added HATU (1 eq) in dry DMF and DIPEA (2 eq). The mixture was stirred at room temperature for 10 min before addition of γ-modified PNA backbone (0.67 eq) in dry DMF. The mixture was stirred overnight or until consumption of the backbone as confirmed by TLC using ninhydrin staining. Upon completion, the reaction was quenched with H_2O, extracted with ethyl acetate and washed with 1M hydrochloric acid (HCl), saturated aqueous sodium bicarbonate ($NaHCO_3$), H_2O, and brine. The organic layer was dried with anhydrous sodium sulfate (Na_2SO_4) and concentrated with rotary evaporation. The crude solid was purified by flash column

chromatography (hexane to ethyl acetate gradient) to give the protected PNA monomer. The purified benzyl-protected monomer was re-dissolved in methanol under N_2. To the solution was added palladium on activated charcoal (7%/wt.) and the N_2 was replaced with a balloon of H_2. The reaction was stirred until complete deprotection as confirmed by TLC. Upon completion, the solution was filtered through celite and concentrated with rotary evaporation to produce the final γ-modified PNA monomer.

Fmoc Lysyl Adenine Monomer (**1**). (43% yield) ^{1}H NMR (400 MHz, DMSO-d6, two rotamers) δ 8.75 (rotamer one, s, 1H) 8.73 (rotamer two, s, 1H) 8.45 (rotamer one, s, 1H) 8.43 (rotamer two, s, 1H) 7.88 (d, 2H) 7.69 (t, 2H) 7.26-7.43 (m, 4H) 6.81 (s, 1H) 6.76 (s, 1H) 5.40 (m, 2H) 5.18 (m, 2H) 4.18-4.36 (m, 3H) 3.81 (m, 1H) 3.49 (m, 2H) 2.87 (m, 2H) 1.00-1.60 (m, 6H) 1.38 (s, 9H) 1.36 (s, 18H). ^{13}C NMR (400 MHz, DMSO-d6) δ 170.78, 170.26, 167.04, 166.58, 156.25, 156.03, 155.64, 153.53, 150.10, 150.02, 148.96, 144.04, 143.91, 140.80, 140.79, 127.80, 127.52, 127.29, 126.94, 125.30, 120.19, 120.14, 83.31, 77.39, 46.95, 29.44, 28.40, 28.22, 27.40, 27.22. HRMS (ESI-TOF) *m/z* 887.3907 (calc'd $[M + H]^+$ = 887.4298).

Fmoc Lysyl Thymine Monomer (**2**). (49% yield) ^{1}H NMR (400 MHz, DMSO-d6, two rotamers) δ 11.30 (rotamer one, s, 1H) 11.28 (rotamer two, s, 1H) 7.88 (d, 2H) 7.68 (t, 2H) 7.41 (t, 2H) 7.32 (t, 2H) 7.21 (s, 1H) 6.77 (m, 1H) 4.63 (m, 2H) 4.45 (s, 1H) 4.30 (m, 2H) 4.21 (m, 2H) 3.92 (m, 2H) 3.35 (m, 2H) 2.88 (m, 2H) 1.72 (rotamer one, s, 3H) 1.69 (rotamer two, s, 3H) 1.19-1.44 (m, 6H) 1.36 (s, 9H). ^{13}C NMR (400 MHz, DMSO-d6) δ 170.32, 167.81, 167.45, 164.43, 156.14, 156.00, 155.62, 151.01, 143.91, 143.83, 140.79, 140.76, 127.66, 127.11, 125.24, 120.17, 108.14, 77.38, 65.34, 47.75, 46.87, 38.29, 29.33, 28.30, 22.90, 22.82, 11.96. HRMS (ESI-TOF) *m/z* 678.3166 (calc'd $[M + H]^+$ = 678.3134).

Fmoc Methyl Cytosine Monomer (**3**). (43% yield) ^{1}H NMR (400 MHz, DMSO-d6) δ 7.95 (d, 1H) 7.87 (d, 2H) 7.68 (d, 2H) 7.40 (m, 3H) 7.33 (t, 2H) 6.79 (t, 1H) 4.84 (m, 1H) 4.67 (m, 1H) 4.26 (m, 4H) 3.93 (m, 2H) 3.48 (m, 2H) 1.48 (s, 18H) 1.01 (d, 3H). ^{13}C NMR (400 MHz, DMSO-d6) δ 168.03, 162.30, 162.22, 155.98, 165.63, 162.11, 149.70, 144.32, 141.14, 128.02, 127.48, 125.65, 120.53, 95.61, 84.92, 64.92, 52.48, 50.41, 48.89, 47.15, 45.68, 27.66, 18.76 HRMS (ESI-TOF) *m/z* 706.3113 (calc'd $[M + H]^+$ = 706.3083).

Fmoc Methyl Thymine Monomer (**4**). (85% yield) ^{1}H NMR (400 MHz, DMSO-d6) δ 11.25 (s, broad, 1H) 7.87 (d, 2H) 7.68 (d, 2H) 7.41 (m, 3H) 7.32 (t, 2H) 7.22 (s, 1H) 4.63 (m, 1H) 4.44 (m, 2H) 4.25 (m, 3H) 3.83 (s, 2H) 3.44 (m, 2H) 1.70 (s, 3H) 0.99 (d, 3H) ^{13}C NMR (400 MHz, DMSO-d6) δ 168.36, 167.50, 164.86, 155.97, 151.46, 144.40, 144.29, 142.63, 141.13, 128.03, 127.51, 125.68, 120.52, 110.00, 108.37, 65.71, 48.26, 47.17, 45.76, 18.87, 12.32. HRMS (ESI-TOF) *m/z* 521.2051 (calc'd $[M + H]^+$ = 521.2031).

Synthesis of 4-(dimethylamino)naphthalimide monomer:

The 4-DMN monomer was synthesized according to an adapted procedure from Saito, et. al.[33]

4-dimethylamino-napthalic anhydride (**5**). 4-bromo-1,8-naphthalic anhydride (1 eq) dissolved in isoamyl alcohol was brought to reflux in an oil bath. 3-Dimethylamino-proprionitrile (4 eq) was added and the mixture was refluxed overnight. The reaction was cooled to room temperature and the precipitate filtered. The precipitate was washed with water and cold hexane and dried under reduced pressure to yield a brown solid in quantitative yield. ^{1}H NMR (400 MHz, $CDCl_3$) δ 8.50 (d, 1H) 8.46 (d, 1H) 8.37 (d, 1H) 7.65 (t, 1H) 7.06 (d, 1H) 3.18 (s, 6H). ^{13}C NMR (400 MHz, $CDCl_3$) δ 161.76, 160.78, 157.98, 135.03, 133.20, 133.00, 125.02, 124.83, 119.19, 113.18, 109.30, 44.69. HRMS (ESI-TOF) *m/z* 242.0834 (calc'd $[M + H]^+$ = 242.0812).

4-dimethylamino-naphthalimide tert-butyl acetate (**6**). To a solution of 4-dimethylamino-napthalic anhydride **5** (36 mmol) and glycine tert-butyl ester (54 mmol) in 180 mL of dry DMF was added DIPEA (108 mmol). The turbid solution was brought to 80 °C and stirred overnight or until full consumption of the anhydride by TLC. Upon completion, the reaction was quenched by addition of 250 mL water and extracted with ethyl acetate (3x250 mL). The organic layer was washed with water and brine, dried with anhydrous sodium sulfate, and concentrated using rotary evaporation. The crude solid was purified by flash column chromatrography (1:1 ethyl acetate:hexane) to yield a yellow solid (78%). ^{1}H NMR (400 MHz, $CDCl_3$) δ 8.50 (d, 1H) 8.40 (d, 1H) 8.36 (d, 1H) 7.59 (t, 1H) 7.02 (d, 1H) 4.80 (s, 2H) 3.05 (s, 6H) 1.46 (9H). ^{13}C NMR (400 MHz, $CDCl_3$) δ 167.40, 164.28, 163.63, 157.20, 133.01, 132.93, 130.45, 125.25, 125.17, 122.58, 114.28, 113.21, 113.11, 81.98, 44.72, 41.96, 28.15. HRMS (ESI-TOF) *m/z* 355.16595 (calc'd $[M + H]^+$ = 355.1652).

4-dimethylamino-naphthalimide acetic acid (**7**). 4-dimethylamino-naphthalimide tert-butyl acetate **6** (18 mmol) was dissolved in a 50% mixture of TFA in DCM (90 mL). After stirring for 3 hours, TLC indicated reaction completion. The reaction was concentrated using rotary evaporation and azeotroped with toluene (3x). The solid was triturated with hexane/DCM, filtered, and the collected solid was dried under reduced pressure to yield the final product as a yellow solid (94%). ^{1}H NMR (400 MHz, DMSO-d6) δ 13.02 (s, broad, 1H) 8.40 (d, 1H) 8.35 (d, 1H) 8.21 (d, 1H) 7.66 (t, 1 H) 7.08 (d, 1H) 4.67 (s, 2H) 3.04 (s, 6H). ^{13}C NMR (400 MHz, DMSO-d6) δ 169.59, 163.31, 162.53, 156.76, 132.53, 131.96, 130.77, 129.66, 124.84, 123.98, 121.67, 112.76, 112.35, 44.34, 40.94. HRMS (ESI-TOF) *m/z* 299.10318 (calc'd $[M + H]^+$ = 299.1026).

Fmoc 4-dimethylamino-naphthalimide (aminoethyl)glycine benzyl ester (**8**). 4-dimethylamino-naphthalimide acetic acid **7** (2.67 mmol) was dissolved in dry DMF (15 mL) under N_2 in a round

bottom flask. The flask was charged with HATU (2.67 mmol) and DIPEA (4.46 mmol). The reaction was stirred for 15 min before addition of Fmoc(aminoethyl)glycine benzyl ester PNA backbone (1.78 mmol) in dry DMF (5 mL). The reaction was stirred for 2.5 h, at which time TLC showed complete consumption of the backbone. Upon completion, the reaction was quenched with H_2O, extracted with ethyl acetate and washed with 1M HCl, saturated $NaHCO_3$, H_2O and brine. The organic layer was dried with anhydrous sodium sulfate and concentrated by rotary evaporation. The crude yellow solid was purified by flash column chromatography (hexane to ethyl acetate gradient) to provide the product as a yellow solid (72%). ^{1}H NMR (400 MHz, $CDCl_3$) δ 8.51 (d, 1H) 8.38 (m, 2H) 7.69 (m, 3H) 7.57 (m, 2H) 7.31 (m, 9H) 7.01 (d, 1H) 6.23 (t, 1H) 5.15 (s, 2H) 5.10 (s, 2H) 4.40 (d, 1H) 4.30 (t, 2H) 4.13 (s, 2H) 3.40-3.70 (m, 4H) 3.05 (s, 6H) ^{13}C NMR (400 MHz, $CDCl_3$) δ 169.81, 168.08, 164.43, 163.83, 157.23, 157.09, 144.20, 141.29, 135.23, 133.12, 131.56, 131.46, 130.57, 128.81, 128.68, 128.46, 128.39, 127.64, 127.13, 125.45, 125.20, 124.80, 122.68, 119.90, 114.41, 113.22, 67.89, 67.34, 49.32, 49.11, 47.29, 44.79, 40.98, 39.66. HRMS (ESI-TOF) *m/z* 711.2901 (calc'd $[M + H]^+$ = 711.2813).

Fmoc 4-dimethylamino-naphthalimide PNA monomer (**9**). Fmoc 4-dimethylamino-naphthalimide (aminoethyl)glycine benzyl ester **8** (1.49 mmol) was dissolved in methanol (25 mL) under N_2. Palladium on activated charcoal (7%/wt.) was added to the solution. The N_2 was replaced by H_2 and the reaction was stirred overnight, after which TLC showed full conversion to product. The reaction was filtered through celite and concentrated using rotary evaporation to provide the product as a yellow solid in quantitative yield. ^{1}H NMR (400 MHz, DMSO-d6, two rotamers) δ 8.52 (rotamer one, d, 1H) 8.46 (rotamer two, d, 1H) 8.42 (rotamer one, d, 1H) 8.37 (rotamer two, d, 1H) 8.31 (rotamer one, d, 1H) 8.24 (rotamer two, d, 1H) 7.87 (rotamer one, t, 3H with Fmoc) 7.76 (rotamer two, t, 1H) 7.70 (d, 2H) 7.66 (d, 2H) 7.54 (t, 1H) 7.20 (rotamer one, d, 1H) 7.14 (rotamer two, d, 1H) 4.98 (s, 2H) 4.80 (s, 2H) 4.34 (d, 2H) 4.27 (t, 1H) 3.56 (t, 2H) 3.15 (m, 2H) 3.10

(rotamer one, s, 6H) 3.07 (rotamer two, s, 6H). ^{13}C NMR (400 MHz, DMSO-d6) δ 167.39, 166.82, 136.39, 162.67, 156.75, 156.46, 156.13, 143.94, 140.75, 132.41, 131.85, 130.70, 129.75, 127.62, 127.09, 125.20, 124.99, 124.19, 122.05, 120.13, 112.88, 65.64, 46.77, 46.39, 44.39, 44.36, 38.26. HRMS (ESI-TOF) *m/z* 621.2399 (calc'd $[M + H]^+$ = 621.2344).

PNA oligomer synthesis

PNA was synthesized on a Biotage SP Wave semi-automatic peptide synthesizer. Synthesis began by down-loading 50mg of a rink amide MBHA resin (0.52 mmol/g) with 5 μmols of the first Fmoc PNA monomer or Fmoc-Lys(Boc)-OH using HATU (1.2 eq), DIPEA (1.2 eq), and 2,6-lutidine (1.2 eq) in 200 μL dry NMP for 1 hour at room temperature followed by 1 hour of capping using a solution of 9% acetic anhydride/13% 2,6-lutidine in DMF. Successive couplings were performed using microwave assistance at 75 °C for 6 min with Fmoc PNA monomer (5 eq), HATU (5eq), DIPEA (5 eq) and 2,6-lutidine (5 eq) in 400 μL dry NMP. After coupling, capping (2x5 min with 1mL capping solution), washing (3x1.1 mL DMF, 3x1.1 mL DCM, then 3x1.1 mL DMF), deprotection (3x2 min with 1mL 25% piperidine/DMF), and washing (same as previous) completed a coupling cycle. All steps were monitored for completion by Kaiser test. Monomer coupling efficiency was monitored by absorbance at 301 nm of the dibenzofulvene-piperidine adduct using a Nanodrop 2000 spectrophotometer. Upon completion of synthesis, cleavage was performed twice using 500 μL of cleavage solution (95% TFA/2.5% triisopropylsilane/2.5% H_2O) for 1 h. The crude oligomer was collected by ether precipitation and purified by reverse-phase HPLC using an Agilent Eclipse XDB-C18 5 μm, 9.4 x 250 mm column at 60°C with a flow rate of 2 mL/min, monitored at 260 nm using a linear gradient (10-40%) of 0.1% TFA/acetonitrile in 0.1% TFA/water. Identity was confirmed by ESI-TOF mass spectrometry.

Melting Temperature Analysis of PNA Strands

Samples containing 5 μM PNA and 5 μM complementary DNA or miRNA-21 were prepared from stock solutions in 1x PBS. The samples were transferred to an 8-cell quartz microcuvette with a 1 cm pathlength. A Shimadzu UV-1800 spectrophotometer equipped with a temperature controller and Julabo CORIO CD water circulator was used for the measurement. Absorbance was monitored at 260 nm from 25-95 °C at a rate of 0.5 °C/min. Melting temperatures were calculated by the first derivative method using a total of three independent trials.

Preparation of PNA amphiphile assemblies

In order to form uniform assemblies, samples of PNA dissolved in water or 1x PBS were heated to 95 °C for 30 min. The samples were then cooled to room temperature and incubated for at least 1 h before analysis.

PNA amphiphile CMC determination using internal 4-DMN monomer

The critical micelle concentration (CMC) of PNA-A was determined by the fluorescence response of the internal 4-DMN monomer. Samples of PNA-A, control PNA-C, and fully deprotected 4-DMN monomer ranging in concentration from 125 μM–0.0.061 μM in 1%DMSO/H_2O were prepared from stock solutions. DMSO was used to initially dissolve the monomer, then stock solutions were prepared in H_2O to a final DMSO content of 1% in each sample. Each sample was treated for amphiphile assembly as previously stated. Samples were then transferred to a 384-well clear-bottom plate for analysis on a Biotek Cytation5 plate reader (higher concentrations) or to a 50 μL quartz cuvette for analysis by a Horiba Scientific Dual-FL fluorometer (lower concentrations). Fluorescence measurements at 550 nm were collected using an excitation of 458 nm. Absorbance was also measured at 458 nm to correct for any changes in concentration between PNA samples and the monomer. A plot of the fluorescence enhancement of the PNA samples over the monomer versus concentration was created using GraphPad Prism

software and used to estimate the CMC. A semi-logarithmic fit to the data provided equations for the upper and lower portions of the curve, which were then compared to determine a CMC value of 317 nM.

Characterization of assemblies by TEM

Samples of PNA at 1mM and 100 μM were prepared in H_2O from stock solutions. Assemblies were formed as previously stated. 3.5 μL of sample was spotted onto a 200-mesh formvar/carbon-coated copper grid for 2 min before wicking with filter paper. 3.5 μL of a fresh 1% uranyl acetate stain solution was then spotted onto the grids for 30 sec before wicking with filter paper. The grids were allowed to dry at room temperature for 30 min before imaging using a Hitachi HT7700 transmission electron microscope.

Size distribution determination from TEM

Images were analyzed using the NIH ImageJ software. Particle diameters were measured manually by setting the scale of the image to the scale bar. Lines were drawn and measured in triplicate for each particle that had clear boundaries without overlap in order to accurately determine an average diameter for each particle. A total of 128 particles were measured and a histogram of the data using 12 bins for size was produced using the GraphPad Prism software.

Determination of size using dynamic light scattering

Samples of PNA were prepared in water to a concentration of 500 μM. The samples were heated to 95°C for 30 min, followed by sonication at 50°C for 10 min and incubation at RT for 1 hour to create uniform assemblies. Sizes were measured using a Particulate Systems NanoPlus DLS nano particle analyzer and automically generated by the NanoPlus software.

Confirmation of binding of complementary DNA to PNA-A by CD

DNA and RNA samples were purchased from Integrated DNA Technologies. Circular dichroism was used to confirm binding and therefore disruption of PNA amphiphile assemblies. Samples of PNA were prepared at 200 μM in 1x PBS. Assemblies were formed as previously stated. DNA stocks at concentrations of 100 μM, 200 μM, 300 μM, and 400 μM were prepared in 1x PBS. 30 μL of PNA was mixed with 30 μL of DNA stocks to a final concentration of 100 μM PNA and DNA concentrations of 50 μM, 100 μM, 150 μM, and 200 μM in 1x PBS. Samples were incubated for 1 h before being analyzed by a JASCO J-1500 circular dichroism spectrometer. Data points were collected every 1 nm from 190-300 nm using a continuous scanning mode of 200 nm/min at 23.5°C. Samples containing a scrambled DNA sequence were prepared in the same manner and analyzed simultaneously.

Confirmation of binding of miRNA-21 to PNA-A by CD

Samples were prepared similarly to analysis by DNA. PNA-A samples of 200 μM in water were prepared as previously described. A 200 μM stock of miRNA-21 was added to the samples in water to a final concentration of 100 μM PNA and 100 μM miRNA-21. The samples were incubated for 1 h before being analyzed.

PNA amphiphile disassembly by 4-DMN fluorescence

Samples of PNA-A at 11.11 μM in 1.1xPBS were prepared and the assemblies formed as previously stated. Complementary and scrambled DNA stocks ranging from 25 μM–200 μM were prepared and 5 μL of each was added to the appropriate PNA sample to a final concentration of 10 μM PNA and 2.5 μM-20 μM DNA in 1xPBS. After addition, samples were incubated for 1 hour before being transferred to a 384-well plate and analyzed using a Biotek Cytation5 plate reader. Fluorescence measurements at 550 nm were collected using an excitation of 458 nm.

PNA amphiphile disassembly by complementary DNA on TEM

Samples of 400 μM PNA-A in 1x PBS were prepared from stock solutions. Assemblies were formed as previously stated. To the samples was added complementary DNA or a scrambled DNA sequence in 1x PBS for a final concentration of 200 μM PNA-A and 200 μM DNA. Samples were incubated at room temperature for 1 h before preparation for TEM using the same procedure described above.

PNA amphiphile disassembly by complementary RNA on TEM

Samples of 200 μM PNA-A in water were prepared from stock solutions. Assemblies were formed as previously stated. To the samples was added a 200 μM stock of miRNA-21 in water to a final concentration of 100 μM PNA-A and 100 μM miRNA-21. The samples were incubated at room temperature for 1 h before preparation for TEM.

Supporting Information

Supporting information available: characterization of monomers and PNA sequences and additional TEM images.

Acknowledgements

This work was supported by the National Science Foundation (DMR 1822262 J.M.H.). The authors also acknowledge the Robert P. Apkarian Integrated Electron Microscopy Core and NMR Research Center at Emory University for access to instruments and technical assistance, and Mr. Steve Knutson for helpful input on the writing of this manuscript.

Declaration of Interests:

The authors declare no competing interests.

References:

(1) Seeman, N. C.; Sleiman, H. F. DNA Nanotechnology. *Nat. Rev. Mater.* **2018**, *3* (1), 17068. https://doi.org/10.1038/natrevmats.2017.68.
(2) Sato, K.; Hendricks, M. P.; Palmer, L. C.; Stupp, S. I. Peptide Supramolecular Materials for Therapeutics. *Chem. Soc. Rev.* **2018**, *47* (20), 7539–7551. https://doi.org/10.1039/C7CS00735C.
(3) Habibi, N.; Kamaly, N.; Memic, A.; Shafiee, H. Self-Assembled Peptide-Based Nanostructures: Smart Nanomaterials toward Targeted Drug Delivery. *Nano Today* **2016**, *11* (1), 41–60. https://doi.org/10.1016/j.nantod.2016.02.004.
(4) Peterson, A. M.; Heemstra, J. M. Controlling Self-Assembly of DNA-Polymer Conjugates for Applications in Imaging and Drug Delivery. *Wiley Interdiscip. Rev. Nanomedicine Nanobiotechnology* **2015**, *7* (3), 282–297. https://doi.org/10.1002/wnan.1309.
(5) Kwak, M.; Herrmann, A. Nucleic Acid Amphiphiles: Synthesis and Self-Assembled Nanostructures. *Chem. Soc. Rev.* **2011**, *40* (12), 5745. https://doi.org/10.1039/c1cs15138j.
(6) Zhang, F.; Nangreave, J.; Liu, Y.; Yan, H. Structural DNA Nanotechnology: State of the Art and Future Perspective. *J. Am. Chem. Soc.* **2014**, *136* (32), 11198–11211. https://doi.org/10.1021/ja505101a.
(7) Egholm, M.; Buchardt, O.; Nielsen, P. E.; Berg, R. H. Peptide Nucleic Acids (PNA). Oligonucleotide Analogs with an Achiral Peptide Backbone. *J. Am. Chem. Soc.* **1992**, *114* (5), 1895–1897. https://doi.org/10.1021/ja00031a062.
(8) Nielsen, P. E. Peptide Nucleic Acid. A Molecule with Two Identities. *Acc. Chem. Res.* **1999**, *32* (7), 624–630. https://doi.org/10.1021/ar980010t.
(9) Dueholm, K. L.; Peterson, K. H.; Jensen, D. K.; Egholm, M.; Nielsen, P. E.; Buchardt, O. Peptide Nucleic Acid (PNA) with a Chiral Backbone Based on Alanine. *Bioorg. Med. Chem. Lett.* **1994**, *4* (8), 1077–1080. https://doi.org/10.1016/S0960-894X(01)80684-3.
(10) Egholm, M.; Buchardt, O.; Christensen, L.; Behrens, C.; Freier, S. M.; Driver, D. A.; Berg, R. H.; Kim, S. K.; Norden, B.; Nielsen, P. E. PNA Hybridizes to Complementary Oligonucleotides Obeying the Watson–Crick Hydrogen-Bonding Rules. *Nature* **1993**, *365* (6446), 566–568. https://doi.org/10.1038/365566a0.
(11) Demidov, V. V; Potaman, V. N.; Frank-Kamenetskii, M. D.; Egholm, M.; Buchardt, O.; Sonnichsen, S. H.; Nielsen, P. E. Stability of Peptide Nucleic Acids in Human Serum and Cellular Extracts. *Biochem. Pharmacol.* **1994**, *48* (6), 1310–1313.
(12) Nielsen, P. E.; Haaima, G.; Lohse, A.; Buchardt, O. Peptide Nucleic Acids(PNAs) Containing Thymine Monomers Derived from Chiral Amino Acids: Hybridization and Solubility Properties OfD-Lysine PNA. *Angew. Chemie Int. Ed. English* **1996**, *35* (17), 1939–1942. https://doi.org/10.1002/anie.199619391.
(13) Sforza, S.; Tedeschi, T.; Corradini, R.; Marchelli, R. Induction of Helical Handedness and DNA Binding Properties of Peptide Nucleic Acids (PNAs) with Two Stereogenic Centres. *European J. Org. Chem.* **2007**, *2007* (35), 5879–5885. https://doi.org/10.1002/ejoc.200700644.
(14) Dragulescu-Andrasi, A.; Rapireddy, S.; Frezza, B. M.; Gayathri, C.; Gil, R. R.; Ly, D. H. A Simple γ-Backbone Modification Preorganizes Peptide Nucleic Acid into a Helical Structure. *J. Am. Chem. Soc* **2006**, *128* (31), 10258–10267. https://doi.org/10.1021/JA0625576.
(15) Yeh, J. I.; Shivachev, B.; Rapireddy, S.; Crawford, M. J.; Gil, R. R.; Du, S.; Madrid, M.; Ly, D. H. Crystal Structure of Chiral ΓPNA with Complementary DNA Strand: Insights into the Stability and Specificity of Recognition and Conformational Preorganization. *J. Am. Chem. Soc.* **2010**, *132* (31), 10717–10727. https://doi.org/10.1021/ja907225d.
(16) Zhou, P.; Wang, M.; Du, L.; Fisher, G. W.; Waggoner, A.; Ly, D. H. Novel Binding and Efficient Cellular Uptake of Guanidine-Based Peptide Nucleic Acids (GPNA). *J. Am. Chem. Soc* **2003**, *125* (23), 6878–6879. https://doi.org/10.1021/JA029665M.

(17) Sahu, B.; Chenna, V.; Lathrop, K. L.; Thomas, S. M.; Zon, G.; Livak, K. J.; Ly, D. H. Synthesis of Conformationally Preorganized and Cell-Permeable Guanidine-Based γ-Peptide Nucleic Acids (ΓGPNAs). *J. Org. Chem.* **2009**, *74* (4), 1509–1516. https://doi.org/10.1021/jo802211n.
(18) Manicardi, A.; Fabbri, E.; Tedeschi, T.; Sforza, S.; Bianchi, N.; Brognara, E.; Gambari, R.; Marchelli, R.; Corradini, R. Cellular Uptakes, Biostabilities and Anti-MiR-210 Activities of Chiral Arginine-PNAs in Leukaemic K562 Cells. *ChemBioChem* **2012**, *13* (9), 1327–1337. https://doi.org/10.1002/cbic.201100745.
(19) Dose, C.; Seitz, O. Single Nucleotide Specific Detection of DNA by Native Chemical Ligation of Fluorescence Labeled PNA-Probes. *Bioorg. Med. Chem.* **2008**, *16* (1), 65–77. https://doi.org/10.1016/J.BMC.2007.04.059.
(20) Englund, E. A.; Wang, D.; Fujigaki, H.; Sakai, H.; Micklitsch, C. M.; Ghirlando, R.; Martin-Manso, G.; Pendrak, M. L.; Roberts, D. D.; Durell, S. R.; et al. Programmable Multivalent Display of Receptor Ligands Using Peptide Nucleic Acid Nanoscaffolds. *Nat. Commun.* **2012**, *3* (1), 614. https://doi.org/10.1038/ncomms1629.
(21) Englund, E. A.; Appella, D. H. Synthesis of γ-Substituted Peptide Nucleic Acids: A New Place to Attach Fluorophores without Affecting DNA Binding. *Org. Lett.* **2005**, *7* (16), 3465–3467. https://doi.org/10.1021/OL051143Z.
(22) De Costa, N. T. S.; Heemstra, J. M. Evaluating the Effect of Ionic Strength on Duplex Stability for PNA Having Negatively or Positively Charged Side Chains. *PLoS One* **2013**, *8* (3), e58670. https://doi.org/10.1371/journal.pone.0058670.
(23) Vernille, J. P.; Kovell, L. C.; Schneider, J. W. Peptide Nucleic Acid (PNA) Amphiphiles: Synthesis, Self-Assembly, and Duplex Stability. *Bioconjug. Chem.* **2004**, *15* (6), 1314–1321. https://doi.org/10.1021/BC049831A.
(24) Marques, B. F.; Schneider, J. W. Sequence-Specific Binding of DNA to Liposomes Containing Di-Alkyl Peptide Nucleic Acid (PNA) Amphiphiles. *Langmuir* **2005**, *21* (6), 2488–2494. https://doi.org/10.1021/LA047962U.
(25) Lau, C.; Bitton, R.; Bianco-Peled, H.; Schultz, D. G.; Cookson, D. J.; Grosser, S. T.; Schneider, J. W. Morphological Characterization of Self-Assembled Peptide Nucleic Acid Amphiphiles. *J. Phys. Chem. B* **2006**, *110* (18), 9027–9033. https://doi.org/10.1021/JP057049H.
(26) Kumarswamy, R.; Volkmann, I.; Thum, T. Regulation and Function of MiRNA-21 in Health and Disease. *RNA Biol.* **2011**, *8* (5), 706–713. https://doi.org/10.4161/rna.8.5.16154.
(27) Nielsen, P. E.; Egholm, M. An Introduction to Peptide Nucleic Acid. *Curr. Issues Molec. Biol.* **1999**, *1* (2), 89–104.
(28) Kleiner, R. E.; Brudno, Y.; Birnbaum, M. E.; Liu, D. R. DNA-Templated Polymerization of Side-Chain-Functionalized Peptide Nucleic Acid Aldehydes. *J. Am. Chem. Soc* **2008**, *130* (14), 4646–4659. https://doi.org/10.1021/JA0753997.
(29) Loving, G.; Imperiali, B. A Versatile Amino Acid Analogue of the Solvatochromic Fluorophore 4- *N,N* -Dimethylamino-1,8-Naphthalimide: A Powerful Tool for the Study of Dynamic Protein Interactions. *J. Am. Chem. Soc.* **2008**, *130* (41), 13630–13638. https://doi.org/10.1021/ja804754y.
(30) Manna, A.; Rapireddy, S.; Sureshkumar, G.; Ly, D. H. Synthesis of Optically Pure ΓPNA Monomers: A Comparative Study. *Tetrahedron* **2015**, *71* (21), 3507–3514. https://doi.org/10.1016/j.tet.2015.03.052.
(31) Porcheddu, A.; Giacomelli, G.; Piredda, I.; Carta, M.; Nieddu, G. A Practical and Efficient Approach to PNA Monomers Compatible with Fmoc-Mediated Solid-Phase Synthesis Protocols. *European J. Org. Chem.* **2008**, *2008* (34), 5786–5797. https://doi.org/10.1002/ejoc.200800891.
(32) Wu, Y.; Xu, J.-C. Synthesis of Chiral Peptide Nucleic Acids Using Fmoc Chemistry. *Tetrahedron* **2001**, *57* (38), 8107–8113. https://doi.org/10.1016/S0040-4020(01)00789-X.

(33) Ikeda, H.; Nakamura, Y.; Saito, I. Synthesis and Characterization of Naphthalimide-Containing Peptide Nucleic Acid. *Tetrahedron Lett.* **2002**, *43* (32), 5525–5528. https://doi.org/10.1016/S0040-4039(02)01164-4.
(34) Kollar, J.; Hrdlovic, P.; Chmela, S.; Sarakha, M.; Guyot, G. Synthesis and Transient Absorption Spectra of Derivatives of 1,8-Naphthalic Anhydrides and Naphthalimides Containing 2,2,6,6-Tetramethylpiperidine; Triplet Route of Deactivation. *J. Photochem. Photobiol. A Chem.* **2005**, *170* (2), 151–159. https://doi.org/10.1016/J.JPHOTOCHEM.2004.07.021.
(35) Grimm, J. B.; English, B. P.; Chen, J.; Slaughter, J. P.; Zhang, Z.; Revyakin, A.; Patel, R.; Macklin, J. J.; Normanno, D.; Singer, R. H.; et al. A General Method to Improve Fluorophores for Live-Cell and Single-Molecule Microscopy. *Nat. Methods* **2015**, *12* (3), 244–250. https://doi.org/10.1038/nmeth.3256.
(36) Feagin, T. A.; Shah, N. I.; Heemstra, J. M. Convenient and Scalable Synthesis of Fmoc-Protected Peptide Nucleic Acid Backbone. *J. Nucleic Acids* **2012**, *2012*, 1–5. https://doi.org/10.1155/2012/354549.
(37) Pabisch, S.; Feichtenschlager, B.; Kickelbick, G.; Peterlik, H. Effect of Interparticle Interactions on Size Determination of Zirconia and Silica Based Systems - A Comparison of SAXS, DLS, BET, XRD and TEM. *Chem. Phys. Lett.* **2012**, *521*, 91–97. https://doi.org/10.1016/j.cplett.2011.11.049.
(38) Souza, T. G. F.; Ciminelli, V. S. T.; Mohallem, N. D. S. A Comparison of TEM and DLS Methods to Characterize Size Distribution of Ceramic Nanoparticles. In *Journal of Physics: Conference Series*; Institute of Physics Publishing, 2016; Vol. 733, p 012039. https://doi.org/10.1088/1742-6596/733/1/012039.
(39) Domingos, R. F.; Baalousha, M. A.; Ju-Nam, Y.; Reid, M. M.; Tufenkji, N.; Lead, J. R.; Leppard, G. G.; Wilkinson, K. J. Characterizing Manufactured Nanoparticles in the Environment: Multimethod Determination of Particle Sizes. *Enironmental Sci. Technol.* **2009**, *43* (19), 7277–7284. https://doi.org/10.1021/es900249m.
(40) Faccini, A.; Tortori, A.; Tedeschi, T.; Sforza, S.; Tonelli, R.; Pession, A.; Corradini, R.; Marchelli, R. Circular Dichroism Study of DNA Binding by a Potential Anticancer Peptide Nucleic Acid Targeted Against the MYCN Oncogene. **2008**, *500* (April 2007), 494–500. https://doi.org/10.1002/chir.
(41) Sharma, C.; Awasthi, S. K. Versatility of Peptide Nucleic Acids (PNAs): Role in Chemical Biology, Drug Discovery, and Origins of Life. *Chem. Biol. Drug Des.* **2017**, *89* (1), 16–37. https://doi.org/10.1111/cbdd.12833.

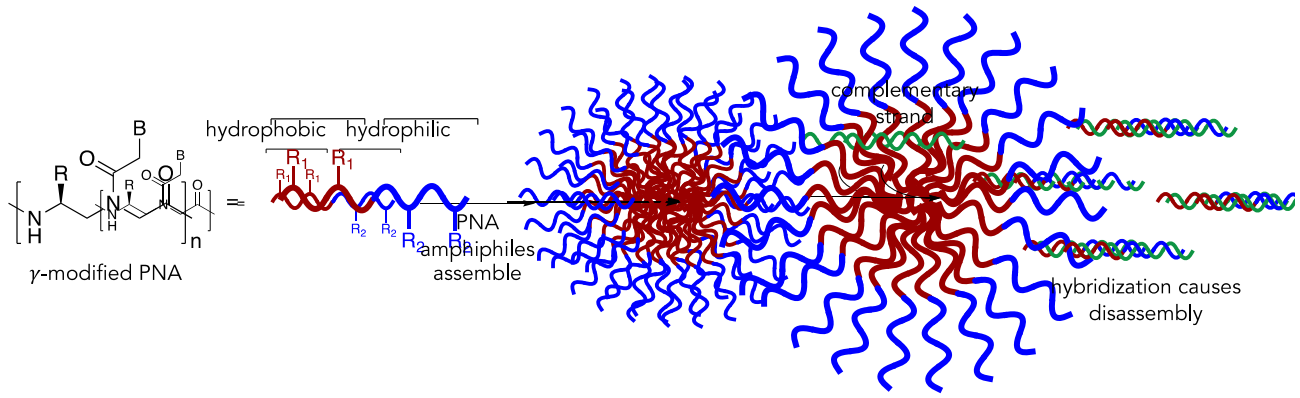
hydrophobic
hydrophilic
γ-modified PNA
PNA amphiphiles assemble
complementary strand
hybridization causes disassembly

TOC Graphic